Available online at www.sciencedirect.com
SCIENCE DIRECT®
Biochimie 86 (2004) 893–901
BIOCHIMIE
www.elsevier.com/locate/biochi

The effects of amino acid replacements of glycine 20 on conformational stability and catalysis of staphylococcal nuclease

Yanming Feng [a], Sun Huang [a], Wenzheng Zhang [b], Zonghao Zeng [b], Xiajuan Zou [c], Lijun Zhong [c], Jiarou Peng [c], Guozhong Jing [a,*]

[a] *National Laboratory of Biomacromolecules, Institute of Biophysics, Chinese Academy of Sciences, Beijing 100101, PR China*
[b] *Center for Structural and Molecular Biology, Institute of Biophysics, Chinese Academy of Sciences, Beijing 100101, PR China*
[c] *Medical and Health Analytical Center, Peking University, Beijing, PR China*

Received 3 June 2004; received in revised form 11 October 2004; accepted 12 October 2004

Available online 04 November 2004

Abstract

Staphylococcal nuclease (SNase) is a well-established model for protein folding studies. Its three-dimensional structure has been determined. The enzyme, Ca^{2+}, and DNA or RNA substrate form a ternary complex. Glycine 20 is the second position of the first β-turn of SNase, which may serve as the folding initiation site for the SNase polypeptide. To study the role of Gly20 in the conformational stability and catalysis of SNase, three mutants, in which Gly20 was replaced by alanine, valine, or isoleucine, were constructed and studied by using circular dichroism spectra, intrinsic and ANS-binding fluorescence spectra, stability and activity assays. The mutations have little effect on the conformational integrity of the mutants. However, the catalytic activity is reduced drastically by the mutations, and the stability of the protein is progressively decreased in the order G20A<G20V<G20I. Kinetic analysis indicates that the mutant enzymes G20A and G20V show almost 20-fold higher K_m^{Ca} values than the wild-type enzyme, and the value for G20I is more than 50-fold higher. K_A^{Ca} values indicate more than 17.5-fold weaker binding of Ca^{2+} to the G20A and G20V mutants, and more than 39-fold weaker to the G20I mutant, compared to wild-type SNase. The above results suggest that the substitutions at Gly20 cause significantly weaker binding of Ca^{2+} in both the binary enzyme-Ca^{2+} complex and the ternary complex. However, there is little difference in the values of K_m^{DNA} and K_S^{DNA} between the mutants and the wild-type enzyme, suggesting that the substitutions at Gly20 have little effect on the binding of DNA substrates to the enzyme. Consistent with the changes in K_m^{Ca} and K_A^{Ca}, the mutant enzymes G20A, G20V and G20I show about 10^3-, 10^4- and 10^5-fold lower K_{Cat} values than the wild-type enzyme, respectively. These results suggest that Gly20 plays an important role in maintaining a suitable conformation at the active site of the enzyme.

Keywords: Staphylococcal nuclease; Amino acid substitutions; Kinetic analysis; Conformational stability

1. Introduction

Staphylococcal nuclease (SNase, EC 3.1.31.1) is a small, globular protein of 149 residues. X-ray crystallography [1–3] and nuclear magnetic resonance (NMR) [4–6] have been used to determine the three-dimensional structure of SNase. It consists of a five-stranded β-barrel and three α-helices, and unfolding induced by heat or chemical denaturant is reversible. The hydrolysis of DNA and RNA by the enzyme is completely dependent on the presence of Ca^{2+}, and pdTp (deoxythymidine 3′, 5′-bisphosphate) is a competitive inhibitor of the enzyme. The structure of the enzyme-Ca^{2+}-pdTp complex has been proposed to be a good model for the productive complex of enzyme, Ca^{2+}, and substrate [1,2,7].

Analysis of mutant proteins with single amino acid substitutions can provide a general strategy for quantifying the contributions of individual residues to protein folding and stability. Many studies have focused on changes in the relative stabilities of single and multiple mutants and on the effects of amino acid substitutions on the structure, stability, and catalysis of SNase mutants [7–18]. Most of the mutations, such as substitutions of the large hydrophobic amino

* Corresponding author. National Laboratory of Biomacromolecules, Institute of Biophysics, Chinese Academy of Sciences, Datun Road 15, Beijing 100101, PR China. Tel.: +86-10-64879271; fax: +86-10-64840672.
E-mail address: jinggzh@sun5.ibp.ac.cn (G. Jing).

0300-9084/$ - see front matter © 2004 Elsevier SAS. All rights reserved.
doi:10.1016/j.biochi.2004.10.005

acids [8] and the polar, uncharged amino acids [9] with alanine and glycine, result in a decrease in stability of the mutants to varying extents. However, hydrophobic substitutions at Tyr 27, which is the first position of a type I′ β-turn (Tyr27-Gln30), produce stable mutants [18]. Substitution mutations at the active site, such as Asp21Glu [10,11], Asp40Gly [12], and Glu43Ser [13], lead to a decrease in catalysis.

An NMR study of a large SNase fragment, Δ131Δ, has reported that the three-stranded antiparallel β-sheet (β_1-β_2-β_3) persisted at high urea concentration [19]. Native-like β-turn conformations of the segments Ile18-Asp21 and Tyr27-Gln30 were observed in the partially folded fragments SNase1-110, SNase1-121 and SNase1-135 fragments, based on the native-like dispersion of the cross-peaks in the corresponding 2D HSQC spectra [20]. The segments Ile18-Asp21 and Tyr27- Gln30 are in the β-hairpins formed by strands 1 and 2, and 2 and 3, respectively. Study of the conformational states of three N-terminal short fragments, SNase1-20, SNase1-28 and SNase1-36, has been performed using circular dichroism (CD) and NMR in aqueous solution or in a trifluoroethanol (TFE)-H_2O mixture. The sequence region Ala17-Thr22 of SNase1-28 displays a localized propensity to form a turn-like conformation in both aqueous solution and TFE-H_2O. The conformational ensemble of SNase1-36 in aqueous solution includes populated turn-like conformations localized in sequence regions Ala17-Thr22 and Tyr27-Gln30 [21]. These results suggests that these sequence regions, which form regular secondary structural features in the native protein (β-turn 1 and β-turn 2), may serve as the folding initiation sites of the SNase polypeptide.

To examine the effect of amino acid substitutions in β-turn 1 on conformational integrity, stability, and catalysis of SNase, Gly20 was chosen as a probe. It is the second position of the first β-turn of SNase, which comprises residues 19–22 and links the antiparallel strands 1 and 2 [2,3]. The reasons for examining this site are threefold. Gly20 is the second residue of the β-turn 1, which is one of the proposed sites for initiation of folding as described above. Secondly, as Gly20 has no side chain, rotation around both φ and ψ is much less restricted. The solvent accessible area for Gly20 indicates that it is in a not very exposed position. Substitution of Gly20 with bulky residues will increase the steric size of side chain, plus the addition of a β carbon will greatly restrict the local φ–ψ angles available to the chain, and so a significant perturbation of the first β-turn structure may result. Thirdly, this residue is near the active site of SNase, but it is not directly involved in the catalysis of the enzyme. In this paper, wild-type staphylococcal nuclease and three mutants in which Gly20 was replaced by Alanine, Valine, and Isoleucine, were constructed and their structural properties compared using circular dichroism spectra, intrinsic and ANS-binding fluorescence spectra, stability and activity assays. The results show that the mutations have little effect on the conformational integrity of the mutants. However, the stability of the proteins is progressively decreased in the order G20A>G20V>G20I, and the catalytic activity is reduced drastically by the mutations. Kinetic analysis indicates that decrease in the catalytic activity is principally related to reducing Ca^{2+} binding.

2. Materials and methods

2.1. Construction of plasmids for the expression of SNase and its mutants

Genes of SNase (wild-type) and three substitution mutants (G20A, G20V and G20I) were prepared by site-directed mutagenesis using pBVS-1 [22] as the template. The N-terminal and C-terminal PCR primers for SNase were: 5′-CAT GCC ATG GCA ACT TCA ACT AAA AAA TTA C-3′ and 5′-ACC GCT CGA GTT GAC CTG AAT CAG CGT TGT-3′, respectively. For the substitution mutants, in addition to the above N- and C-terminal primers used for SNase, the mutagenesis primers were 5′-A TTT AAC CGT ATC AGC ATC AAT C-3′, 5′-A TTT AAC CGT ATC AAC ATC AAT C-3′ and 5′-A TTT AAC CGT ATC GAT ATC AAT C-3′ to make megaprimers for mutants G20A, G20V, and G20I, respectively. The PCR products were inserted into the *Nco*I and *Xho*I sites of pET-28a after digestion with the same enzymes, and the entire gene of each mutant was sequenced. The plasmids were then transformed into BL21 (DE3) for the expression of SNase and its mutants. All the proteins were expressed in *E. coli* cells with a C-terminal hexahistidine tag. In this case, SNase and its mutants contain a total of 158 residues including a Met_i encoded by the initiation codon and a C-terminal Leu-Glu- $(His)_6$ sequence in which Leu and Glu were created by the *Xho*I site.

2.2. Expression and purification of SNase and its mutants

E. coli BL21 (DE3) cells harboring the appropriate recombinant plasmid were cultured at 37 °C overnight. The culture was then diluted 50-fold with fresh pre-warmed LB medium supplemented with 50 μg/ml kanamycin, and incubated at 37 °C until a turbidity of 0.6 at 600 nm was obtained prior to induction by 0.4 mM IPTG for 4 h. Protein was purified using a modified method, which includes the procedure of protein refolding on a column [23]. Briefly, the cell pellet was collected by centrifugation at 6000*g* for 20 min at 4 °C, and then resuspended in a lysis buffer (20 mM Tris–HCl, pH 8.0, 0.5 M NaCl, 5 mM imidazole, 8 M urea). The mixture was ultrasonicated and then centrifuged at 27,000*g* for 30 min at room temperature. The supernatant was directly applied onto a 5 × 1 cm^2 of chelating Sepharose Fast Flow column at a flow rate of 1.0 ml/min, which had been charged with Ni^{2+} according to the producer's protocol (Amersham Biosciences) and equilibrated with the lysis buffer. The column was washed first with 50 ml of the lysis buffer, followed by 50 ml of a washing buffer (20 mM Tris–HCl, pH 8.0, 0.5 M

NaCl, 60 mM imidazole, 8 M urea). Afterwards, refolding was performed using a linear 8–0 M urea gradient, starting with the washing buffer and ending with the refolding buffer (20 mM Tris–HCl, pH 8.0, 0.5 M NaCl, 60 mM imidazole). The gradient buffer volume was 200 ml and the flow rate was 0.3 ml/min. Finally, the protein was eluted using an elution buffer (20 mM Tris–HCl, pH 8.0, 0.5 M NaCl, 200 mM imidazole), and then dialyzed against Tris buffer (20 mM Tris–HCl, pH 7.4) and stored at –70 °C for later use.

Each purified protein appeared as a single band on a 15%-SDS polyacrylamide gel. The protein concentration was determined by the method of Bradford [24].

2.3. Circular dichroism measurements

Circular dichroism (CD) spectra were obtained at 20 °C using a Jasco J-720 spectropolarimeter with a 1 mm path length quartz cuvette. The protein concentration in the samples was 10 μM for far-UV CD (250–200 nm) and 100 μM for near-UV CD (320–250 nm), in 20 mM Tris–HCl, pH 7.4. The CD spectral data represent the average of four scans after correction for the buffer baseline and were reported as mean residue ellipticity ([θ]).

2.4. Fluorescence measurements

Intrinsic fluorescence emission spectra and ANS-binding fluorescence spectra of the proteins were measured at 25 °C using a Hitachi F-4500 fluorescence spectrophotometer with slit width of 5 nm. For the intrinsic fluorescence measurements, the excitation wavelengths were 295 and 285 nm for tryptophan and tyrosine, respectively. The concentration of each protein was 3 μM in 20 mM Tris–HCl, pH 7.4. For measurement of ANS-binding fluorescence, 1-anilinonaphthalene-8-sulfonate (1,8-ANS, Sigma) was used as a hydrophobic fluorescence probe. The excitation wavelength was 350 nm, and each sample contained 5 μM protein and 50 μM ANS in 20 mM Tris–HCl, pH 7.4.

2.5. Urea induced denaturation

Urea induced denaturation of SNase and its mutants were measured by monitoring the change of intrinsic fluorescence of the tryptophan residue at position 140. Each sample containing 5 μM of protein in 20 mM Tris–HCl, pH 7.4, with different concentrations of urea, was incubated overnight at 25 °C. The measurements were performed at 25 °C on a Hitachi F-4500 fluorescence spectrophotometer. The sample was excited at 295 nm, and the emission intensity at 325 nm was recorded.

To measure the difference in stabilities ($\Delta\Delta G'_{H_2O}$) of the mutants, the apparent equilibrium constant for denaturation (K_{app}) was determined by monitoring the intrinsic fluorescence of the single tryptophan residue at position 140 as a function of denaturant concentration according to the equation $K_{app} = (I_n - I)/(I - I_d)$ where I is the measured intrinsic fluorescence, I_n is the extrapolated value of fluorescence for the native state, and I_d is the extrapolated value for the denatured state. The value of K_{app} was extrapolated linearly to a denaturant concentration of zero, and $\Delta G'_{H_2O}$ is given by the equation $\Delta G' = -RT\ln K_{app}$ and $\Delta(\Delta G) = \Delta G$ (mutant) – ΔG (SNase) [25].

2.6. Enzymatic activity assay and kinetics measurements

The enzyme activity was measured at 25 °C using a Hitachi-2010 spectrophotometer by observing the change in absorbance at 260 nm [26]. One unit of enzymatic activity was defined as the amount of enzyme causing a change of 1.0 absorbance unit/min at 260 nm in a 1.0-cm cell. The reaction mixture contained 20 mM Tris–HCl, pH 7.4, 10 mM $CaCl_2$, and 50 μg/ml denatured salmon sperm DNA.

The kinetic parameters of SNase and its mutants were obtained by analyzing the initial velocity of reactions according to the method described by Serpersu et al. [12].

Limited proteolysis of SNase and its mutants using endoproteinase Glu-C in the presence and absence of pdTp, and peptide electrophoresis

There are 12 potential cleavage sites for the special endoproteinase, Glu-C, along the sequence of SNase as shown in Fig. 1. Comparison of their susceptibilities to the endoproteinase in SNase and its mutants may provide useful information about the conformational state of the protein. Glu-C (sequencing grade) was purchased from Sigma. Only glutamyl bonds of proteins are cleaved by the protease in

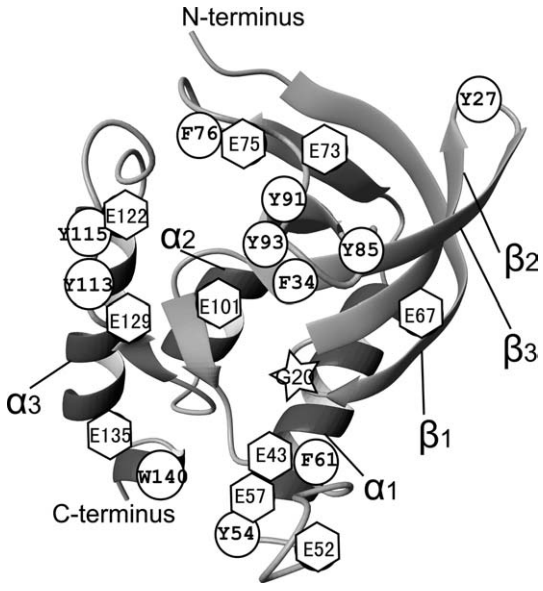

Fig. 1. Potential cleavage sites for endoproteinase Glu-C and the positions of aromatic residues in the SNase molecule. There are 12 potential cleavage sites for Glu-C along the sequence of SNase. They are located at positions 43, 52, 57, 67, 73, 75, 101, 122, 129, 135, 142, and 151 that is an additional cleavage site created by *Xho*1 site for inserting the genes into pET-28a vector. Here, only 10 cleavage sites are indicated. The Glu142 and Glu151 are omitted as they are not visible in the crystal structure of the enzyme. The positions of 11 aromatic amino acid residues and Gly20 residue are also indicated.

ammonium bicarbonate buffer pH 7.8 [27,28]. SNase and its mutants were first incubated at 4 °C overnight in 60 mM ammonium bicarbonate buffer, pH 7.8, 2 mM EDTA, in the presence and absence of pdTp (molar ratio of pdTp/protein = 10) and 10 mM $CaCl_2$. Then Glu-C was added to start the reactions at 37 °C. The total reaction mixture volume, 100 µl, contained 150 µg of protein sample with an optimal enzyme-to-substrate ratio of 1:5000. Aliquots were drawn from the reaction mixture at different times for later electrophoresis, mixed with the eletrophoresis loading buffer, and then immediately heated in a boiling water bath for 10 min to stop the reaction. Peptide electrophoresis was carried out according to the method described by Schägger et al. [29].

2.8. Sample preparation and peptide molecular mass measurement by using MALDI-TOF-MS

The initial events during the digestion of the protein sample were traced by setting the digestion time according to the peptide electrophoresis results. The protein samples for MALDI-TOF-MS measurements were first precipitated by the addition of PMSF to 1 mM and TCA (trichloracetic acid) to 10%, after digestion as described above, and then recovered by centrifugation at 13,000*g* at 4 °C for 20 min. The dried sample was dissolved in 40 µl solution containing 50% acetonitrile and 0.1% TFA (trifluoroacetic acid) for MALDI-MS analysis. A freshly prepared solution of α-cyano-4-hydroxycinnamic acid (10 mg/ml) in 70% acetonitrile and 0.1% TFA was mixed with the same volume of the above sample solution. A total of 1.0 µl of sample mixture was applied to the MALDI target and allowed to dry. MALDI-TOF mass spectra were acquired on an AXIMA-CFP plus mass spectrometer equipped with a 337.1-nm nitrogen laser. Data from 100 laser shots were averaged for each spectrum. Each spectrum was internally calibrated across the 3–20 kDa mass range.

3. Results

3.1. Circular dichroism spectra of SNase and its mutants

Far-UV CD spectra were used to assess the secondary structure, especially the α-helical content. The appearance of two negative peaks at 208 and 222 nm in the CD spectrum is usually considered to be typical of α-helical structure in a protein [30]. As shown in Fig. 2, the far-UV CD spectra of the mutants show two negative peaks at 208 and 222 nm and there is a little difference between the spectra of SNase and its mutants, which indicates that the substitution mutations at Gly20 have no significant effect on the secondary structure of the nuclease.

Fig. 3 shows the near-UV CD spectra of SNase and its mutants, which reflect the asymmetry of the environment of aromatic amino acids. Changes in the spectra, especially around 277 nm, are usually considered to be indicative of

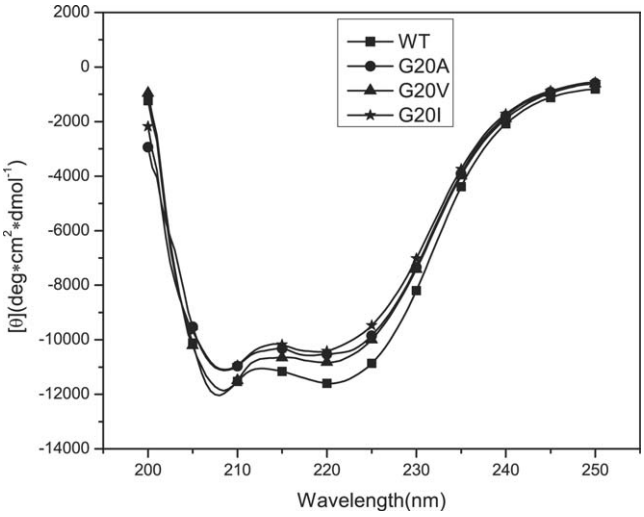

Fig. 2. Far-UV CD spectra of SNase and its mutants.

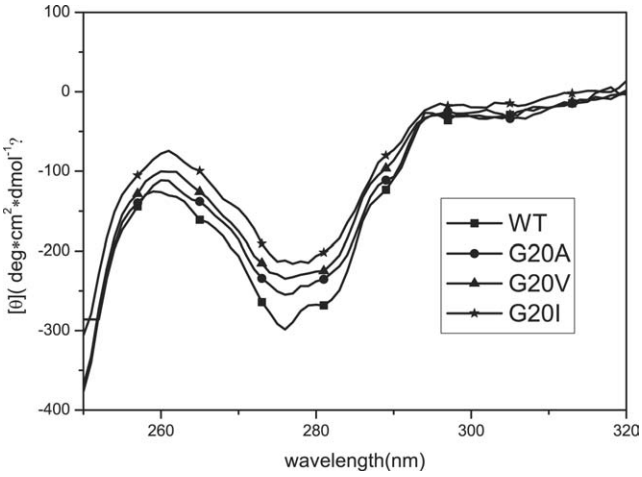

Fig. 3. Near-UV CD spectra of SNase and its mutants.

changes in the protein tertiary structure [30]. Compared with SNase, $[\theta]_{277\ nm}$ values of G20A, G20V, and G20I are decreased by 12.5 ± 1.7%, 19.8 ± 1.8%, and 26.7 ± 3.2%, respectively. These changes suggest that the substitutions at Gly20 have an effect on the specific packing of aromatic groups in the tertiary structure of the mutants.

3.2. Fluorescence spectra of SNase and its mutants

There is a single tryptophan residue at position 140 (Trp140) at the C-terminus of SNase, which is buried in a hydrophobic environment [1,2]. Changes in the intrinsic tryptophan fluorescence spectra of the excitation at 295 nm reflect changes in the local environment of the tryptophan residue. As shown in Fig. 4, the intrinsic tryptophan fluorescence spectra for SNase and its mutants are almost identical, suggesting that the substitutions at Gly20 cause no changes in the local hydrophobic environment around Trp140. As shown in Fig. 1, there are seven tyrosine residues in SNase. Intrinsic tyrosine fluorescence spectra were also measured, by excitation at 285 nm. These spectra also show no obvious difference between SNase and its mutants (data not shown).

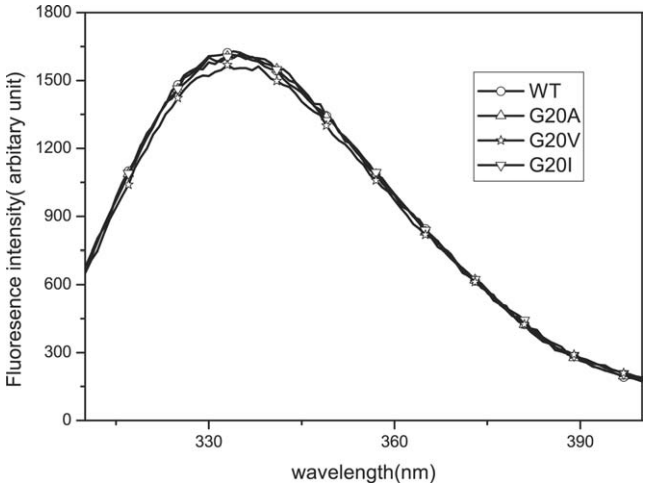

Fig. 4. Tryptophan fluorescence emission spectra of SNase and its mutants.

3.3. ANS-binding fluorescence spectra of SNase and its mutants

ANS is used as a hydrophobic fluorescence probe to measure changes in the surface hydrophobicity of proteins. The difference in surface hydrophobicity reflects changes in the exposure of hydrophobic side chains, which in turn reflects the degree of folding of a protein molecule. Fig. 5 shows the fluorescence emission spectra of ANS in the presence of SNase and its mutants. There is no detectable difference in the ANS fluorescence spectra in the presence of SNase and its mutants, suggesting that the substitutions at Gly20 do not cause any change in the surface hydrophobicity of the protein.

3.4. Catalytic activity and kinetics of SNase and its mutants

The specific and relative activities of SNase and its mutants are shown in Table 1. The catalytic activity is reduced drastically by the three mutations. The mutant G20A retains

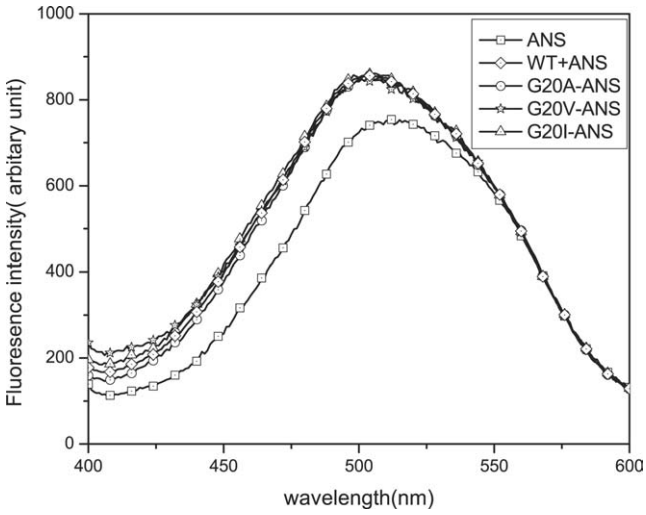

Fig. 5. ANS fluorescence spectra in the presence of SNase and its mutants.

Table 1
Specific and relative activities of SNase and its mutants

Protein	Specific activity (ΔOD_{260} min^{-1} μmol^{-1})	Relative activity (%)
Snase	5714 ± 272	100
G20A	119 ± 6	2.0
G20V	26 ± 1.2	0.45
G20 I	12 ± 0.7	0.21

Activity of the proteins was measured as described in the text. Relative activity = [(specific activity of a given protein)/(specific activity of SNase)] × 100%.

only 2% of native activity, while the mutants G20V and G20I retain only 0.45% and 0.21%, suggesting that Gly20 is a very important residue for maintaining the active conformation of the nuclease.

A detailed kinetic analysis of SNase and its mutants was performed according to the method described by Serpersu et al. [13]. A comparison of the kinetic parameters for wild-type SNase and its substitution mutants (Table 2) indicates that at saturating levels of DNA, the mutant enzymes G20A and G20V show almost 20-fold higher K_m^{Ca} values than the wild-type enzyme, and G20I more than 50-fold. The K_A^{Ca} values, which represent the K_m of Ca^{2+} extrapolated to zero [DNA], indicate more than 17.5-fold weaker binding of Ca^{2+} to the G20A and G20V mutants, and more than 39-fold to the G20I mutant than to the wild-type SNase, respectively. The above results suggest that the substitutions at Gly20 cause significantly weaker binding of Ca^{2+} to the mutants in both the binary enzyme-Ca^{2+} complex and in the ternary complex. However, there is little difference in the value of K_m^{DNA} and K_s^{DNA} between the mutants and the wild-type enzyme, suggesting that the substitutions at Gly20 have little effect on the binding of DNA substrates to the mutants. The value of K_{cat} represents the catalytic efficiency of enzyme. As shown in Table 2, the mutant enzymes G20A, G20V and G20I have about 10^3-, 10^4- and 10^5-fold lower K_{Cat} values than the wild-type enzyme, respectively, indicating that the substitutions at Gly20 decrease the catalytic efficiency drastically. As the hydrolysis of DNA or RNA by the enzyme is completely dependent on the presence of Ca^{2+}, the loss of the catalytic efficiency for the mutants is likely to be related to the decrease in affinity of the mutants for Ca^{2+}.

3.5. Urea induced unfolding of SNase and its mutants

Urea induced unfolding of SNase and its mutants was measured by monitoring the changes in the fluorescence emission intensity at 325 nm. The changes in the intrinsic tryptophan fluorescence of SNase and its mutants during unfolding in urea are shown in Fig. 6. It can be seen that the denaturation midpoints for G20A, G20V, and G20I are at 1.5, 1.1, and 0.82 M urea, respectively, while the denaturation midpoint for SNase is at 2.0 M urea. These results indicate that the substitutions at Gly20 clearly destabilize the protein.

The differences in the stabilities of SNase and its mutants were also estimated. As shown in Table 3, Gly20 substitution

Table 2
Comparison of kinetic parameters for SNase and its mutants

Enzyme	K_m^{Ca} (μM) [a]	K_A^{Ca} (μM) [b]	K_m^{DNA} (μg/ml) [c]	K_s^{DNA} (μg/ml) [d]	V_{max} (ΔAbs μg^{-1} min^{-1})	K_{cat} (ΔAbs μg^{-1} min^{-1} M^{-1}) [e]	Relative TN
Snase	113 ± 16	510 ± 61	3.57 ± 0.855	19.7 ± 1.2	0.731 ± 0.082	3.87×10^9	1
G20A	2128 ± 165	986 ± 701	3.22 ± 0.67	17.9 ± 0.7	0.217 ± 0.071	5.16×10^6	1.33×10^{-3}
G20V	005 ± 383	8872 ± 1090	1.52 ± 0.75	13.3 ± 1.1	0.086 ± 0.043	3.03×10^5	7.83×10^{-5}
G20I	026 ± 737	19885 ± 2012	2.91 ± 1.44	16.2 ± 0.9	0.090 ± 0.054	2.29×10^4	5.92×10^{-6}

[a] K_m^{Ca} is the Michaelis constant for Ca^{2+} at saturating [DNA].
[b] K_A^{Ca} is the K_m of Ca^{2+} extrapolated to zero [DNA].
[c] K_m^{DNA} is the Michaelis constant for DNA at saturating [Ca^{2+}].
[d] K_s^{DNA} is the K_m for DNA extrapolated to zero [Ca^{2+}].
[e] K_{cat} was calculated from the formula $K_{cat} = V_{max}/[E]_t$, where $[E]_t$ is the molar concentration of enzyme.

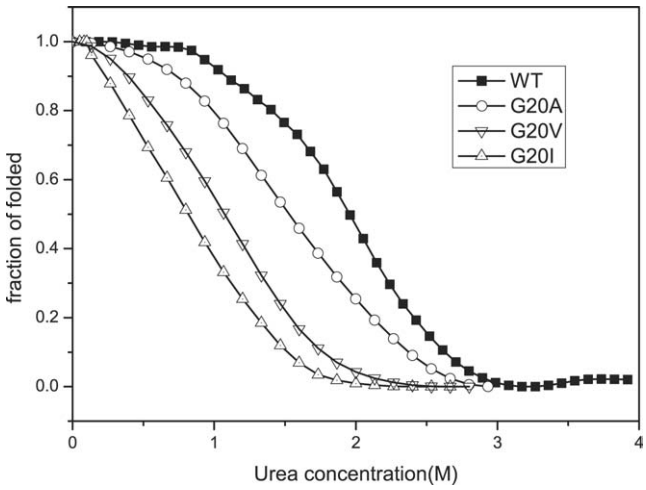

Fig. 6. Changes in the intrinsic tryptophan fluorescence of SNase and its mutants in different concentrations of urea. The fraction change in the intrinsic fluorescence at 325 nm for tryptophan was taken to indicate the extent of protein unfolding.

Table 3
Parameters characterizing the urea-induced unfolding of SNase and its mutants

Protein	$[urea]_{1/2}$ (M) [a]	ΔG [b] (kcal/mol)	$\Delta(\Delta G)$ [c] (kcal/mol)
SNase	2.0	3.38 ± 0.07	0.00
G20A	1.5	2.59 ± 0.05	–0.79
G20V	1.1	2.12 ± 0.08	–1.26
G20I	0.8	1.77 ± 0.07	–1.61

[a] Midpoint urea concentration in molar.
[b] ΔG values were obtained as described in the text.
[c] $\Delta(\Delta G) = \Delta G$ (a given mutant protein) – ΔG (SNase).

mutations result in a decrease in protein stability of 0.79 kcal/mol for G20A, 1.26 kcal/mol for G20V and 1.61 kcal/mol for G20I. These results indicate that Gly20 contributes significantly to the overall stability of the nuclease. The effect of substitution mutations at Gly20 on the conformational stability increases with increasing size of side chain, from G20A to G20V and to G20I.

3.6. Stability detection of SNase and its mutants by using limited proteolysis by Glu-C

It is known that there is a clear-cut correlation between protease susceptibility and conformational stability of proteins, and the initial proteolytic events are the most critical for evaluating the conformational features of proteins [31–36]. The effect of the substitution mutations on the stability of the proteins was also detected by using limited proteolysis, as described in the Section 2. In Fig. 7, A1, B1, C1 and D1 show the peptide electrophoresis patterns of SNase and its mutants after digestion with Glu-C for different times in the absence of ligands. Compared with SNase (A1), each of the mutants (G20A, G20V, and G20I) is more susceptible to Glu-C hydrolysis (B1, C1, D1). It is notewor-

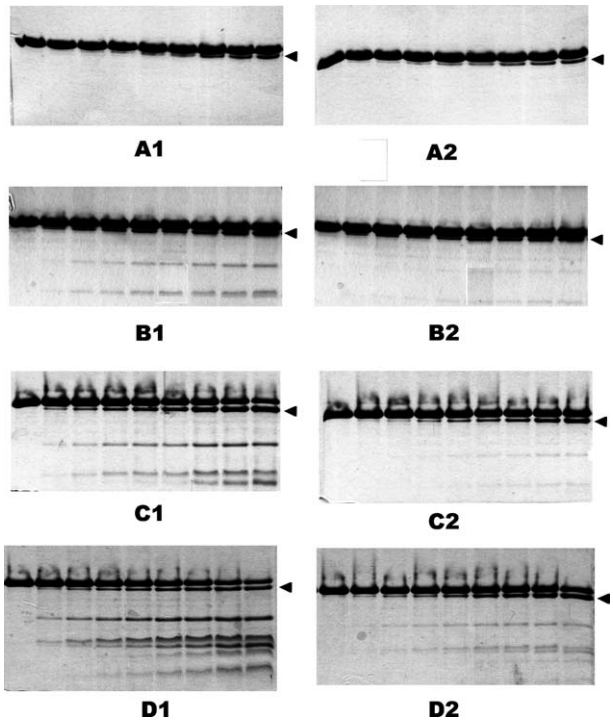

Fig. 7. Peptide electrophoresis patterns of SNase and its mutants in the absence and presence of pdTp and Ca^{2+} after digestion with endoproteinase Glu-C for different times. Experimental conditions are described in the text. A1, B1, C1, D1 denote the digested SNase, G20A, G20V and G20I in the absence of pdTp and Ca^{2+}, respectively, A2, B2, C2, D2 denote the digested SNase, G20A, G20V and G20I in the presence of pdTp and Ca^{2+}, respectively. The digestion times are from left to right: 0, 2, 5, 10, 20, 40, 75, 120 and 180 min. The arrows (3) indicate the polypeptide bands of M_i-E151. The M_i-E151 segment appears for both mutants and SNase, indicating that the E151-H152 site is accessible to Glu-C in all cases. Ligand binding does not significantly protect the site from Glu-C attack.

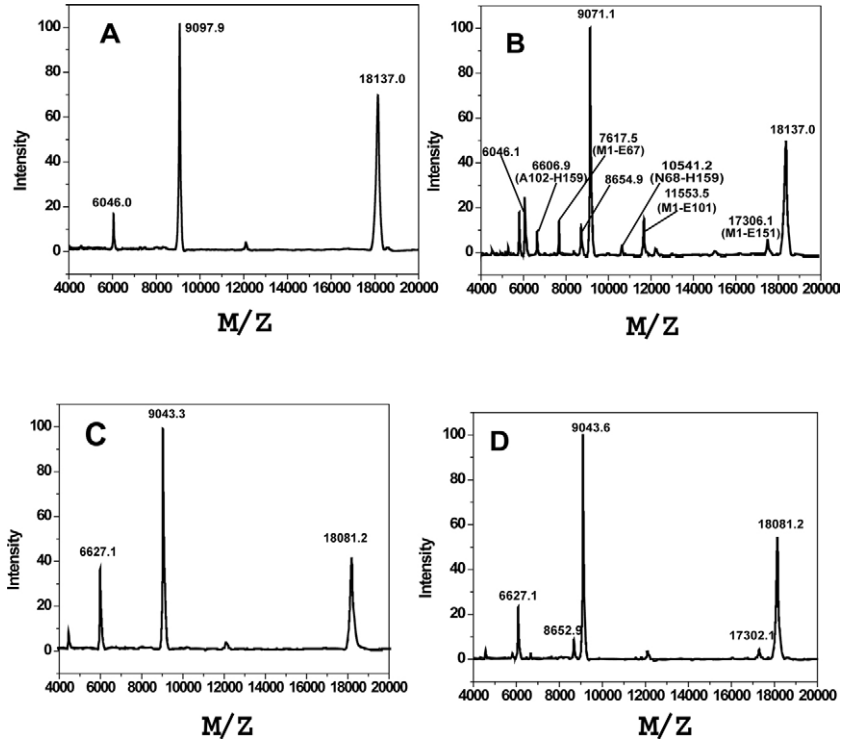

Fig. 8. MALDI-TOF mass spectra of SNase and G20I digested with endoproteinase Glu-C for different times. (A) G20I digested with Glu-C for 0 min. The three peaks at *m/z* 18137.0, 9097.9, and 6046.0 are observed, which correspond to singly, doubly, and triply protonated intact G20I, respectively. (B) G20I digested with Glu-C for 10 min. The peaks at *m/z* 7617.5, 10541.2, 11553.5, 6606.9, and 17306.1 correspond to M_i-E67, N68-H158, M_i-E101, A102-H158 and M_i-E151 segments, respectively. The additional peak at *m/z* 8654.9 corresponds to the doubly protonated M_i-E151 polypeptide segment. (C) SNase digested with Glu-C for 0 min. The three peaks at m/z 18081.2, 9043.3, and 6027.1 are observed, which correspond to singly, doubly, and triply protonated intact SNase, respectively. (D) SNase digested with Glu-C for 10 min. The mass spectrum is the same as (C), except that the two additional peaks appear at *m/z* 13702.1 and 8652.9, corresponding to the singly and doubly protonated M_i-E151 polypeptide segment, respectively.

thy that the susceptibility of the mutants to Glu-C hydrolysis increases from G20A to G20V and to G20I, which correlates well with the steric size of the substituted residues (the sizes for Ala, Val, and Ile are 88.6, 140.0, and 166.7 $Å^3$, respectively). Since there is a clear-cut correlation between protease susceptibility and conformational stability [33,34,36], the differences in the susceptibility reflect the difference in the conformational stability. In Fig. 7, B2, C2 and D2 show the peptide electrophoresis patterns of G20A, G20V, and G20I, respectively, after digestion with Glu-C for different times in the presence of ligands, respectively. Compared with B1, C1 and D1, the ligand binding improves the stabilities of the mutants to some extent.

3.7. Analysis of the conformational state of SNase and its mutants by using mass spectrometry with limited proteolysis

The above results show that the substitutions at Gly20 make the mutants more susceptible to Gly-C hydrolysis. In order to know the structural basis of the changes, mass spectrometry measurements were performed after digestion of SNase and its mutants with Glu-C. The MALDI-TOF mass spectra of G20I digested with Glu-C for different times are shown in Fig. 8. Fig. 8A shows the mass spectrum of G20I digested with Glu-C for 0 min. There are three peaks at *m/z* 18137.0, 9097.9 and 6046.0 corresponding to singly, doubly and triply protonated intact G20I, respectively. The mass spectrum of G20I digested with Glu-C for 10 min, Fig. 8B, has peaks at *m/z* 7617.5, 10541.2, 11553.5, 6606.9, and 17306.1 which correspond to M_i-E67, N68-H158, M_i-E101, A102-H158, and M_i-E151 segments, respectively. The spectrum indicates that there are only three cleavage sites (E67-N68, E101-A102 and E151-H152) cleaved, which are located in the C-terminal part of α-helix 1, the middle of α-helix 2 and the C-terminus of G20I created by the *Xho*I site and His_6 tag, respectively. The peaks that correspond to M_i-E67, N68-H158, M_i-E101, and A102-H158 segments that are observed for G20I are not observed under the same digestion conditions for native enzyme SNase. The results indicate that the cleavage sites E67-N68 and E101-A102 are more resistant to Glu-C attack in the native enzyme SNase. This clearly suggests the existence of some subtle differences in the conformational state of the proteins, making the two cleavage sites in G20I more exposed to Glu-C attack.

4. Discussion

The X-ray structure of the ternary enzyme-Ca^{2+}-pdTp complex reveals that a single Ca^{2+} is liganded to the protein through the side chain carboxylates of Asp21, Asp40, and the

backbone carbonyl oxygen of Thr41. The side chain of Glu43 is bridged by water molecules to both the Ca^{2+} and the 5′-phosphate of the nucleotide and is thought to play the role of a general base in the cleavage of the 5′-phosphate [1,2,7]. Gly20 is the second residue of the first β-turn in SNase, which is not intimately involved in the catalytic process. However, as described above, the substitutions of Gly20 with Ala, Val, or Ile drastically reduce the catalytic activity of the mutants. A comparison of the kinetic parameters (Table 2) indicates that the substitutions cause significantly weaker binding of Ca^{2+} to mutants G20A and G20V, and especially to G20I. However, the substitutions have little effect on the affinity of staphylococcal nuclease for the DNA substrate, as may be seen by comparing the values of K_s^{DNA} and K_m^{DNA} for the mutants and SNase. This suggests that the mutations have little effect on the interaction of Glu43 with the DNA substrate in either the binary enzyme-DNA or ternary enzyme-Ca^{2+}-DNA complex. From the above results, we can conclude that it is the much weaker binding of Ca^{2+} to the mutants that results in their loss of catalytic activity. We used the program TURBO to predict the structure of the Gly20 mutants from the X-ray crystal structure of wild-type SNase [37] and refined the predicted structures using the program XPLOR. The results suggest that although the substitution of Ala, Val, or Ile at Gly20 does not affect the β-turn structure of (D19-G20-D21-T22), the additional side chains protrude into a space between the side chains of Ala58 and Thr42, and push them apart. This then enlarges the distance between Asp40 and the β-turn (residues 19–21), and breaks the hydrogen bonding between D21N and T41OG1. These conformational changes could significantly affect the binding of Ca^{2+} to residues Asp40 and Asp21.

As described above, the substitutions at Gly20 have no detectable effect on the intrinsic and ANS-binding fluorescence spectra. However, the substitutions do cause detectable changes in the near-UV CD spectra of the mutants. Compared with SNase, $[\theta]_{277\ nm}$ values of G20A, G20V, and G20I are decreased by 12.5 ± 1.7%, 19.8 ± 1.8%, and 26.7 ± 3.2%. These results suggest that the mutations perturb the specific packing of the aromatic groups in the tertiary structure of the mutants. As shown in Fig. 1, there are 11 aromatic residues along the sequence of SNase and most of them are located in regions of β-sheet or in turns. Introducing bulky residues at Gly20 which is in a relatively buried position could easily induce changes in the asymmetry of the environment of aromatic groups throughout the protein. The subtle differences in conformation may produce differences in the near-UV CD spectra of the mutants, as the near-UV CD spectrum can be sensitive to small changes in tertiary structure of proteins. A similar result was observed when studying an N-terminal fragment of SNase. Deletion of 10 residues from the N-terminus of SNase has little effect on the far-UV CD, intrinsic, and ANS-binding fluorescence spectra. However, an apparent change in the near-UV CD and in the stability of the protein was observed (in preparation). It is noteworthy that the changes in the protein stability, as characterized by urea denaturation and Glu-C hydrolysis, and in the near-UV CD spectra, correlate well with the increase in steric size of the residue substituted at Gly20. These correlations suggest that the disruption of the specific packing of the aromatic groups in SNase leads to destabilization of the mutants. Kinetic analysis shows that the presence of the substrate DNA increases the affinity of the enzymes for Ca^{2+} and vice versa (Table 2). Given that ligand binding increases the stabilities of the mutants, this implies that binding of the DNA substrate and Ca^{2+} contributes to the stability of the enzyme-Ca^{2+}-substrate complex.

Acknowledgements

This work was supported by grants (Nos. G1999075608 and 30170210) from the China Committee for Science and Technology. The authors would like to thank Professor S. Perrett of this laboratory for a critical reading of this paper and helpful suggestions.

References

[1] F.A. Cotton, E.E. Hazen, M.J. Legg, Staphylococcal nuclease: proposed mechanism of action based on structure of enzyme-thymidine 3′, 5′-bisphosphate–calcium ion complex at 1.5 Å resolution, Proc. Natl. Acad. Sci. USA 76 (1979) 2551–2562.

[2] P.J. Loll, E.E. Lattman, The crystal structure of the ternary complex of staphylococcal nuclease, Ca^{2+}, and the inhibitor pdTp, refined at 1.65 Å, Proteins 5 (1989) 183–201.

[3] T.R. Hynes, R.O. Fox, The crystal structure of staphylococcal nuclease refined at 1.7 Å resolution, Proteins 10 (1991) 92–105.

[4] P.A. Evans, C.M. Dobson, R.A. Kautz, G. Hatfull, R.O. Fox, Proline isomerism in staphylococcal nuclease characterized by NMR and site-directed mutagenesis, Nature 329 (1987) 266–268.

[5] T.A. Alexandrescu, A.P. Hinck, J.L. Markley, Coupling between local structure and global stability of a protein: mutants of staphylococcal nuclease, Biochemistry 29 (1990) 4516–4525.

[6] M.D. Jacobs, R.O. Fox, Staphylococcal nuclease folding intermediate characterized by hydrogen exchange and NMR spectroscopy, Proc. Natl. Acad. Sci. USA 91 (1994) 449–453.

[7] E.H. Serpersu, D. Shortle, A.S. Mildvan, Kinetic and magnetic resonance studies of effects of genetic substitution of a Ca^{2+}-liganding amino acid in staphylococcal nuclease, Biochemistry 25 (1986) 68–77.

[8] D. Shortle, W.E. Stites, A.K. Meeker, Contributions of the large hydrophobic amino acids to the stability of staphylococal nuclease, Biochemistry 29 (1990) 8033–8041.

[9] S.M. Green, A.K. Meeker, D. Shortle, Contributions of the polar, uncharged amino acids to the stability of staphylococcal nuclease: evidence for mutational effects on the free energy of the denatured state, Biochemistry 31 (1992) 5717–5728.

[10] E.H. Serpersu, D. Shortle, A.S. Mildvan, Kinetic and magnetic resonance studies of active-site mutants of staphylococcal nuclease: factors contributing to catalysis, Biochemistry 26 (1987) 1289–1300.

[11] A.M. Libson, A.G. Gittis, E.E. Lattman, Crystal structures of the binary Ca^{2+} and pdTp complexes and the ternary complex of the Asp^{21}→Glu mutant of staphylococcal nuclease. Implications for catalysis and ligand binding, Biochemistry 33 (1994) 8007–8016.

[12] E.H. Serpersu, D. Shortle, A.S. Mildvan, Kinetic and magnetic resonance studies of effects of genetic substitution of a Ca^{2+}- liganding amino acid in staphylococcal nuclease, Biochemistry 25 (1986) 68–77.
[13] E.H. Serpersu, D.W. Hibler, J.A. Gerlt, A.S. Mildvan, Kinetic and magnetic resonance studies of the glutamate-43 to serine mutant of staphylococcal nuclease, Biochemistry 28 (1989) 1539–1548.
[14] H.M. Chen, T.J. Dimagno, W. Wang, E. Leung, C.H. Lee, S.L. Chan, The effect of Glu75 of staphylococcal nuclease on enzyme activity, protein stability and protein unfolding, Eur. J. Biochem. 261 (1999) 599–609.
[15] I. Shin, A.Y. Ting, P.G. Schultz, Analysis of backbone hydrogen bonding in a β-turn of staphylococcal nuclease, J. Am. Chem. Soc. 119 (1997) 12667–12668.
[16] S. Huang, J.H. Yin, Y.M. Feng, G.Z. Jing, Effect of a specific hydrogen bond (N138D2-Q106O) on conformational integrity, stability, and activity of staphylococcal nuclease, Arch. Biochem. Biophys. 420 (2003) 87–94.
[17] M.R. Eftink, C.A. Ghiron, R.A. Kautz, R.O. Fox, Fluorescence and conformational stability studies of staphylococcal nuclease and its mutants, including the less stable nuclease-concanavalin A hybrids, Biochemistry 30 (1991) 1193–1199.
[18] M.G. Bhat, L.M. Ganley, D.W. Ledman, M.A. Goodman, R.O. Fox, Stability studies of amino acid substitutions at tyrosine 27 of the staphylococcal nuclease beta-barrel, Biochemistry 36 (1997) 12167–12174.
[19] Y. Wang, D. Shortle, The equilibrium folding pathway of staphylococcal nuclease: identification of the most stable chain–chain interactions by NMR and CD spectroscopy, Biochemistry 34 (1995) 15895–15905.
[20] Y. Feng, D. Liu, J. Wang, Native-like partially folded conformations and folding process revealed in the N-terminal large fragments of staphylococcal nuclease: a study by NMR spectroscopy, J. Mol. Biol. 330 (2003) 821–837.
[21] J. Dai, X. Wang, Y. Feng, G. Fan, J. Wang, Searching for folding initiation sites of staphylococcal nuclease: a study of N-terminal short fragments, Biopolymers 75 (2004) 229–241.
[22] G.Z. Jing, L.J. Liu, M.Y. Jiang, Q. Zou, R.Q. He, High-level expression of staphylococcal nuclease R gene in *Escherichia coli*, J. Biotechnol. 22 (1992) 271–282.
[23] Purification and renaturation of recombinant proteins produced in Escherichia coli as inclusion bodies. Application Note 18-1112-1133, Amersham Pharmacia Biotech.
[24] M.M. Bradford, A rapid and sensitive method for the quantitation of microgram quantities of protein utilizing the principle of protein–dye binding, Anal. Biochem. 72 (1976) 248–254.
[25] D. Shortle, A.K. Meeker, Mutant forms of staphylococcal nuclease with altered patterns of guanidine hydrochloride and urea denaturation, Proteins 1 (1986) 81–89.
[26] P. Cuatrecasas, S. Fuchs, C.B. Anfinsen, Catalytic properties and specificity of the extracellular nuclease of *Staphylococcus aureus*, J. Biol. Chem. 242 (1967) 1541–1547.
[27] G.R. Drapeau, Protease from *Staphyloccus aureus*, Methods Enzymol. 45 (1976) 469–475.
[28] G.R. Drapeau, Cleavage at glutamic acid with staphylococcal protease, Methods Enzymol. 47 (1977) 189–191.
[29] H. Schägger, G. Von Jagow, Tricine-sodium dodecyl sulfate-polyacrylamide gel electrophoresis for the separation of proteins in the range from 1 to 100 kDa, Anal. Biochem. 166 (1987) 368–379.
[30] Y.V. Griko, A. Gittis, E.E. Lattman, P.L. Privalov, Residual structure in a staphylococcal nuclease fragment. Is it a molten globule and is it unfolding a first-order phase transition? J. Mol. Biol. 243 (1994) 93–99.
[31] A. Fontana, P. Polverino de Laureto, V. De Filippis, E. Scaramella, M. Zambonin, Probing the partly folded states of proteins by limited proteolysis, Fold. Des. 2 (1997) R17–R26.
[32] P. Polverino de Laureto, V. De Filippis, M. Di Bello, M. Zambonin, A. Fontana, Probing the molten globule state of α-lactalbumin by limited proteolysis, Biochemistry 34 (1995) 12596–12604.
[33] A. Fontana, M. Zambonin, P. Polverino de Laureto, V. De Filippis, A. Clementi, E. Scaramella, Probing the conformational state of apomyoglobin by limited proteolysis, J. Mol. Biol. 266 (1997) 223–230.
[34] R. Cotter, Time-of-flight mass spectrometry for the structural analysis of biological molecules, Anal. Chem. 64 (1992) 1027A–1039A.
[35] E.J. Zaluzec, D.A. Gage, J.T. Watson, Matrix-assisted laser desorption ionization mass spectrometry applications in peptide and protein characterization, Prot. Exp. Purif. 6 (1995) 109–123.
[36] F. Yang, Y. Cheng, J.R. Peng, J.M. Zhou, G.Z. Jing, Probing the conformational state of a truncated staphylococcal nuclease R using time of flight mass spectrometry with limited proteolysis, Eur. J. Biochem. 268 (2001) 4227–4232.
[37] J. Chen, Z. Lu, J. Sakon, W.E. Stites, Increasing the thermostability of staphylococcal nuclease: implications for the origin of protein thermostability, J. Mol. Biol. 303 (2000) 125–130.